European Society of Biomechanics S.M. Perren Award 2012: The external mechanical environment can override the influence of local substrate in determining stem cell fate

Stephen D. Thorpe[a], Conor T. Buckley[a], Andrew J. Steward[a,b], Daniel J. Kelly[a,*]

[a] Trinity Centre for Bioengineering, School of Engineering, Trinity College Dublin, Ireland.

[b] Department of Mechanical Engineering and Bioengineering Graduate Program, University of Notre Dame, IN, USA.

*Corresponding author

Address: Trinity Centre for Bioengineering
School of Engineering
Trinity College Dublin
Ireland

Tel: +353-1-896-3947

Fax: +353-1-6795554

E-mail: kellyd9@tcd.ie

Keywords: Mechanobiology; Mesenchymal stem cell; Cartilage tissue engineering; Dynamic compression; Cell shape.

Word count: 5,312

Abstract

The aim of this study was to explore how cell-matrix interactions and extrinsic mechanical signals interact to determine stem cell fate in response to transforming growth factor-β3 (TGF-β3). Bone marrow derived mesenchymal stem cells (MSCs) were seeded in agarose and fibrin hydrogels and subjected to dynamic compression in the presence of different concentrations of TGF-β3. Markers of chondrogenic, myogenic and endochondral differentiation were assessed. MSCs embedded within agarose hydrogels adopted a spherical cell morphology, while cells directly adhered to the fibrin matrix and took on a spread morphology. Free-swelling agarose constructs stained positively for chondrogenic markers, with MSCs appearing to progress towards terminal differentiation as indicated by mineral staining. MSC seeded fibrin constructs progressed along an alternative myogenic pathway in long-term free-swelling culture. Dynamic compression suppressed differentiation toward any investigated lineage in both fibrin and agarose hydrogels in the short-term. Given that fibrin clots have been shown to support a chondrogenic phenotype *in vivo* within mechanically loaded joint defect environments, we next explored the influence of long term (42 days) dynamic compression on MSC differentiation. Mechanical signals generated by this extrinsic loading ultimately governed MSC fate, directing MSCs along a chondrogenic pathway as opposed to the default myogenic phenotype supported within unloaded fibrin clots. In conclusion, this study demonstrates that external cues such as the mechanical environment can override the influence specific substrates, scaffolds or hydrogels have on determining mesenchymal stem cell fate. The temporal data presented in this study highlights the importance of considering how MSCs respond to extrinsic mechanical signals in the long term.

1. Introduction

Bone marrow derived mesenchymal stem cells (MSCs) could potentially provide an effective cell source for tissue engineering and regenerative medicine applications. MSCs can differentiate along several pathways including the chondrogenic, osteogenic, adipogenic and myogenic lineages (Caplan, 1991). The ability to direct MSC differentiation in a stable and concerted manner is crucial to the success of tissue engineering and regenerative medicine therapies. *In vivo* MSC differentiation down distinct lineages is dependent on cues present in the local microenvironment. While much attention has centred on the use of soluble factors to direct MSC differentiation (Minguell et al., 2001; Pittenger et al., 1999), the role of insoluble signals such as cell shape (McBeath et al., 2004), cell adhesion (Connelly et al., 2008), substrate rigidity (Engler et al., 2006) and mechanical cues from the external environment (Huang et al., 2004) are also significant.

It has long been proposed that mechanical signals can direct the differentiation of MSCs (Carter et al., 1988; Pauwels, 1960; Prendergast et al., 1997); a theory supported by *in vitro* bioreactor studies. In the absence of chondrogenic growth factors, dynamic compressive strain applied to hydrogel encapsulated MSCs has been shown to enhance chondrogenic gene expression (Huang et al., 2004; Li et al., 2010; Pelaez et al., 2009) and matrix synthesis (Kisiday et al., 2009; Li et al., 2010; Mauck et al., 2007). The response of MSCs to both biochemical and biophysical cues is more complex, with reports of the simultaneous application of TGF-β3 and dynamic compression suppressing chondrogenic gene expression (Campbell et al., 2006; Haugh et al., 2011; Steinmetz and Bryant, 2011) and matrix accumulation in the early stages of differentiation (Huang et al., 2010; Thorpe et al., 2008). When cytokine mediated differentiation is permitted to occur prior to the application of dynamic compression, chondrogenic gene expression (Haugh et al., 2011; Mouw et al.,

2007), matrix synthesis (Thorpe et al., 2010) and construct mechanical properties (Huang et al., 2010) are increased.

Cell-matrix interactions also play a key role in regulating stem cell fate. Integrin mediated adhesion to the extracellular matrix has been shown to modulate both chondrogenic (Connelly et al., 2008) and osteogenic (Kundu et al., 2009) MSC differentiation, and may act as a means for mechanotransduction (Kock et al., 2009; Wang et al., 2009). One such natural hydrogel which facilitates integrin binding to ligands present on the scaffold is fibrin (Janmey et al., 2009). Fibrin has been shown to support chondrogenic differentiation (Li et al., 2009; Pelaez et al., 2009), but it similarly facilitates osteogenic (Catelas et al., 2006; Weinand et al., 2006) and myogenic (Nieponice et al., 2007; O'Cearbhaill et al., 2010) differentiation of MSCs.

The exact mechanisms of how biochemical and biophysical cues interact to determine stem cell fate within an environment that can potentially support differentiation along multiple pathways, such as a fibrin clot, have yet to be determined. In an *in vitro* setting, TGF-β has been shown to promote both chondrogenic (Johnstone et al., 1998; Mackay et al., 1998) and myogenic (Jeon et al., 2006; Kinner et al., 2002) MSC differentiation. This switch between chondrogenic and myogenic fates in the presence of TGF-β has been shown to depend on matrix stiffness (Park et al., 2011) and cell shape (Gao et al., 2010). Adherent and well spread MSCs were shown to undergo myogenic differentiation in response to TGF-β3, while cells that were prevented from spreading and flattening underwent chondrogenic differentiation (Gao et al., 2010). *In vivo*, insoluble cues will be provided not only by the substrate and associated changes in cell shape, but also from the external mechanical environment. The aim of this paper is to explore how cell-matrix interactions and extrinsic mechanical signals interact to determine stem cell fate in response to TGF-β. We first hypothesised that cell-substrate interactions in a three dimensional hydrogel would determine

MSC fate in response to TGF-β. Specifically, a hydrogel repressing cell adhesion and spreading (agarose) would encourage the chondrogenic differentiation of MSCs, while a hydrogel promoting cell spreading and cell-cell interactions (fibrin) would support a myogenic phenotype. We next explored how extrinsic mechanical signals, specifically dynamic compression of a substrate shown to support myogenesis, would influence stem cell fate. We hypothesised that the long-term application of dynamic compression would override the effects of the local substrate, suppressing myogenesis and enhancing chondrogenesis of MSCs.

2. Methods

2.1 Cell isolation and expansion

Porcine bone marrow-derived MSCs were isolated as mononuclear cells from the femora of 4 month old porcine donors (~50kg) within 2 hours of sacrifice and plated at 10×10^6 cells in 75cm^2 culture flasks (Nunclon; Nunc, VWR, Dublin, Ireland) to allow for colony formation. MSCs were maintained in high-glucose Dulbecco's modified eagles medium (4.5 mg/mL D-Glucose, 200mM L-Glutamine; hgDMEM) supplemented with 10% foetal bovine serum (FBS), penicillin (100 U/mL)-streptomycin (100 µg/mL) (all GIBCO, Invitrogen, Dublin, Ireland) and amphotericin B (0.25µg/mL; Sigma-Aldrich, Arklow, Ireland) . Cultures were washed in Dulbecco's phosphate buffered saline (PBS) after 72 hrs. When ~75% confluent, MSCs were re-plated at 5×10^3 cells/cm^2 and expanded to passage two in a humidified atmosphere at 37°C and 5% CO_2.

2.2 Agarose and fibrin hydrogel encapsulation

For agarose encapsulation, MSCs were suspended in defined chondrogenic medium (CM) consisting of hgDMEM supplemented with penicillin (100 U/mL)-streptomycin (100

μg/mL) (both GIBCO), 100 KIU/mL aprotinin (Nordic Pharma, Reading, UK), 0.25 μg/mL amphotericin B, 100 μg/ml sodium pyruvate, 40 μg/mL L-proline, 1.5 mg/mL bovine serum albumin, 4.7 μg/mL linoleic acid, 1× insulin–transferrin–selenium, 50 μg/mL L-ascorbic acid-2-phosphate and 100 nM dexamethasone (all Sigma-Aldrich). This cell suspension was mixed with agarose (Type VII; Sigma-Aldrich) in PBS at a ratio of 1:1 at ~40°C, to yield a final agarose concentration of 2% and a cell density of 15×10^6 cells/mL. The agarose-cell suspension was cast between stainless steel plates, allowed cool to 21°C for 30 min., and cored to produce cylindrical constructs (Ø 5mm×3mm thickness).

For fibrin encapsulation, MSCs were suspended in 10,000 KIU/mL aprotinin solution (Nordic Pharma) containing 19 mg/mL sodium chloride and 100 mg/mL bovine fibrinogen type I-S (60-85% protein, ~10% sodium citrate and ~15% sodium chloride; Sigma-Aldrich), which was combined 1:1 with 5 U/mL thrombin in 40 mM $CaCl_2$ (pH 7) and allowed to gel in an agarose mould for 45 min. at 37°C; producing cylindrical constructs (Ø 5mm×3mm thickness) with final concentrations of 50 mg/mL fibrinogen, 2.5 U/mL thrombin, 5,000 KIU/mL aprotinin, 17 mg/mL sodium chloride, 20 mM $CaCl_2$ and 15×10^6 cells/mL. Constructs were maintained in 2.5 mL CM with the addition of either 1 ng/mL or 10 ng/mL TGF-β3 (ProSpec-Tany TechnoGene Ltd., Israel). Media was exchanged every 3 or 4 days and sampled for biochemical analysis. The mechanical properties of both hydrogels were determined according to previous protocol (Buckley et al., 2009) and are presented in Table 1.

2.3 Dynamic compression application

Dynamic compressive loading was applied to constructs as described previously (Thorpe et al., 2010). Intermittent dynamic compression (DC) was applied in an incubator-housed, custom dynamic compression bioreactor, and consisted of a sine wave of 10% strain

amplitude superimposed upon a 1% pre-strain, with a 0.01 N per construct preload at a frequency of 1 Hz for 3 hours/day, 7 days/week for 21 days. MSC seeded fibrin constructs were additionally subjected to DC for 42 days, or delayed dynamic compression (DDC) where loading was applied from day 22 to day 42 of culture.

2.4 Biochemical constituents

Constructs were analysed at day 0 (24 hrs. after cell encapsulation), day 21 and day 42. On removal from culture, construct diameter and wet weight (ww) were recorded and constructs were frozen at -85°C for further analysis. Biochemical content was assessed at each time point as previously described (Thorpe et al., 2010). Samples were digested with papain (125μg/ml) in 0.1 M sodium acetate, 5 mM L-cysteine HCl, 0.05 M EDTA (all Sigma-Aldrich), pH 6.0 at 60°C under constant rotation for 18 hours. DNA content was quantified using the Hoechst Bisbenzimide 33258 dye assay (Sigma-Aldrich) as previously described (Kim et al., 1988). The sulphated glycosaminoglycan (sGAG) content was quantified using the dimethylmethylene blue dye-binding assay (Blyscan; Biocolor Ltd., Northern Ireland). Total collagen content was determined by measuring orthohydroxyproline via the dimethylaminobenzaldehyde and chloramine T assay (Kafienah and Sims, 2004). A hydroxyproline-to-collagen ratio of 1:7.69 was used (Ignat'eva et al., 2007). Cell culture media was analysed for sGAG and collagen as above, and alkaline phosphatase using a commercially available assay kit (Sensolyte pNPP Alkaline Phosphatase, Cambridge Biosciences, UK).

2.5 Cell viability and F-actin cytoskeleton fluorescent imaging

MSC seeded constructs were sectioned to produce a cross section ~1 mm thick perpendicular to the disc face. To assess cell viability, sections were washed in PBS followed by incubation in PBS containing 4μM calcein AM (live cell membrane) and 4μM ethidium homodimer-1 (dead cell DNA; both Cambridge Bioscience, Cambridge, UK). Sections were again washed in PBS and imaged with a Carl Zeiss LSM 510 confocal laser scanning microscope.

F-actin cytoskeletal filaments were visualised using rhodamine 110 conjugated phalloidin (VWR). Constructs were sectioned as described above, fixed in 4% paraformaldehyde overnight and washed in PBS. Cells were permeabilised in 0.5% Triton-X100 (Sigma-Aldrich), rinsed in PBS, and incubated for 1.5 hours in PBS with 1.5% BSA and rhodamine 110 conjugated phalloidin (1:40; 200 U/mL; VWR). Construct slices were again rinsed in PBS and imaged with a Carl Zeizz LSM 510 confocal laser scanning microscope.

2.6 Histology and immunohistochemistry

Constructs were fixed in 4% paraformaldehyde, paraffin embedded and sectioned at 5 μm to produce a cross section perpendicular to the disc face. Sections were cleared in xylene, rehydrated, and stained for sGAG with 1% alcian blue 8GX in 0.1M HCl, for collagen with picro-sirius red, and for calcific deposition with 1% alizarin red (all Sigma-Aldrich). Histochemical assessment of alkaline phosphatase (ALP) activity was performed as previously described (Miao and Scutt, 2002). Deparaffinised hydrated tissue sections were incubated overnight in 1% magnesium chloride in 100mM tris-maleate buffer (pH 9.2) followed by incubation for 2 hours in ALP substrate solution consisting of 100mM tris-maleate buffer (pH 9.2) containing 0.2 mg/mL naphthol AS-MX phosphate and 0.4 mg/mL

Fast Red TR (all Sigma-Aldrich). Sections were rinsed in de-ionized water and mounted in glycerol.

The deposition of collagen type I, collagen type II, collagen type X and α-smooth muscle actin was identified through immunohistochemistry. Sections were enzymatically treated with chondroitinase ABC (Sigma-Aldrich) in a humidified environment at 37°C. Cell membranes were permeabilised in 0.1% Triton-X100. Slides were blocked with goat serum (Sigma-Aldrich) and sections were incubated for 1 hour with the primary antibody (all Abcam, Cambridge, UK) diluted in blocking buffer as specified in Table 2. After washing in PBS, sections were incubated for 1 hour in the secondary antibody, anti-mouse IgG biotin antibody produced in goat (1:133; 2 mg/mL; Sigma-Aldrich) followed by incubation for 1 hour with ExtrAvidin-FITC (1:100; Sigma-Aldrich). Sections were washed several times in PBS, nuclei were counterstained with DAPI (1:500; 1 mg/mL; VWR), and sections mounted using Vectashield (Vector Laboratories, Peterborough, UK). Sections were imaged with an Olympus IX51 inverted fluorescent microscope fitted with an Olympus DP70 camera.

2.7 RNA isolation and real-time reverse transcriptase polymerase chain reaction

Quantitative real-time reverse transcription-polymerase chain reaction (qRT-PCR) was used to determine the relative gene expression changes in chondrogenic and myogenic specific genes in response to the application of dynamic compression for 21 days. Total RNA was extracted from MSC seeded constructs following 21 days of culture. Constructs were harvested directly after the application of dynamic compression, snap frozen in liquid nitrogen, and stored at -85°C for later analysis. Total RNA was isolated from each construct via homogenisation using a rotor-stator homogeniser (Polytron PT 1200 E; Kinematica Inc, Switzerland) in 1 mL TRIzol® reagent followed by chloroform extraction with PureLink™

RNA Mini Kit (Invitrogen). RNA was re-suspended in RNase-free water prior to reverse transcription.

RNA concentrations were determined using the Quant-iT™ RNA assay and a Qubit® fluorometer. 100ng of RNA was reverse transcribed into cDNA using the High Capacity cDNA Reverse Transcription Kit (Applied Biosystems, Paisley, UK). Real-time PCR reactions were carried out in 20µL volumes containing 10µL 2× TaqMan® Universal PCR Master Mix, 5µL nuclease free water, 4µL cDNA template (1ng/µL) and 1µL 20× TaqMan® gene expression assay (primer/probes; FAM dye) as outlined in Table 3 (all Applied Biosystems). Reactions were carried out on an ABI 7500 real-time PCR system (Applied Biosystems) with an amplification profile of 50°C for 2 min., 95°C for 10 min., followed by 40 cycles of denaturation at 95°C for 15 sec. and annealing/amplification at 60°C for 1 min. Quantitative expression of target genes relative to the endogenous control reference gene (GAPDH) and the FS calibrator was carried out using the method as previously described (Livak and Schmittgen, 2001).

2.8 Statistical analysis

Presented are results from one of two replicate studies with unique donors, where *n* refers to the number of constructs analysed for each assay within a given replicate (*n* numbers provided in figure legends). Statistics were performed using MINITAB 15.1 software (Minitab Ltd., Coventry, UK). Where necessary, a Box-Cox transformation was used to normalise data sets. Construct groups were analysed for significant differences using a general linear model for analysis of variance with factors of hydrogel, TGF-β3 concentration, dynamic compression and interactions between these factors examined. Tukey's test for multiple comparisons was used to compare conditions. Significance was accepted at a level of $p \leq 0.05$. Numerical and graphical results are presented as mean ± standard error.

3. Results

3.1 Hydrogel type modulates MSC response to TGF-β3 stimulation

MSCs were encapsulated in agarose or fibrin hydrogels and cultured for 21 days in free-swelling unloaded conditions with the addition of either 1 ng/mL or 10 ng/mL TGF-β3. TGF-β3 concentration was investigated on account of the possibility that MSC response to either substrate or mechanical stimulation could be masked by the stimulus provided by 10 ng/mL TGF-β3. At day 21, F-actin cytoskeletal filaments were stained with phalloidin as an indication of stress fibre formation and cell morphology. MSCs seeded in agarose adopted a spherical cell morphology with some processes evident at day 21, suggesting cell binding to elaborated pericellular matrix (Fig. 1). In fibrin constructs, cells adhered to integrin binding sites present on the fibrin matrix and adopted a spread morphology evident at day 21 (Fig. 1). Evidence of cell-cell interactions were also observed in fibrin that were generally absent in agarose hydrogels. Cell viability staining did not indicate any significant effect of hydrogel type or TGF-β3 concentration on live or dead cell numbers (not shown).

The influence of hydrogel type coupled with TGF-β3 concentration on markers of chondrogenic, endochondral and myogenic differentiation was investigated. While sGAG accumulation and alcian blue staining increased with TGF-β3 concentration in agarose and fibrin ($p<0.0001$; Fig. 2A & 2B), agarose appeared to better support TGF-β3 mediated chondrogenesis; as evidenced by greater sGAG accumulation when supplemented with 10ng/mL TGF-β3 ($p<0.0001$; Fig. 2A). Collagen type II immunofluorescence further confirmed this finding with agarose constructs staining more intensely than fibrin (Fig. 2C). Despite low collagen type II immunofluorescence in fibrin hydrogels, total collagen accumulation was superior in fibrin constructs ($p<0.0001$; Fig. 2A), which stained intensely for collagen type I (Fig 2C).

Alkaline phosphatase (ALP) secretion to the media and staining intensity was greater for agarose encapsulated MSCs than those in fibrin ($p<0.0001$; Fig. 2A & 2B). Though increased TGF-β3 concentration led to increased ALP secretion from agarose ($p<0.001$), the same effect was not observed from fibrin (Fig 2A). Pericellular collagen type X immunofluorescence was evident within the agarose constructs, especially at 1 ng/mL TGF-β3 (Fig. 2C). This co-localised with regions of collagen type I (Fig. 2C) and calcific deposits indicated by alizarin red staining (Fig. 2B); providing evidence of endochondral ossification for agarose encapsulated MSCs in the presence of TGF-β3. Interestingly, regions of more intense ALP activity did not appear to co-localise with alizarin red staining (Fig 2B). In contrast to agarose, fibrin constructs stained negatively for collagen type X (Fig. 2C) and alizarin red (Fig. 2B).

Myogenic differentiation was assessed with immunofluorescent staining for α-smooth muscle actin. While pericellular staining was evident at 1 ng/mL TGF-β3 in agarose constructs, this was not observed with increased TGF-β3 concentration (Fig. 2C). In contrast, a cell layer developed on the surface of fibrin constructs which stained intensely for α-smooth muscle actin and was independent of TGF-β3 concentration (Fig. 2C). When the culture period was extended to 42 days, the intensity of α-smooth muscle actin staining in FS fibrin hydrogels increased while the staining for type II collagen diminished, indicating that fibrin hydrogels preferentially support myogenic differentiation over chondrogenic differentiation (Fig. 5). In addition, fibrin construct diameter reduced significantly with time for both TGF-β3 concentrations, (~6% diameter reduction; $p<0.001$) suggesting the adoption of a contractile phenotype.

3.2 Dynamic compression suppresses both chondrogenesis and myogenesis in agarose and fibrin hydrogels when applied at the onset of TGF-β3 induced differentiation

It has previously been shown that dynamic compression inhibits chondrogenesis of agarose encapsulated MSCs at early time points (Haugh et al., 2011; Thorpe et al., 2008). This inhibition may be modulated by cell attachment to the hydrogel matrix. Hence, it was initially hypothesised that substrate mediated alterations in cell shape and attachment would modulate the response to dynamic compression; specifically that such mechanical cues would not suppress chondrogenesis of MSCs embedded in fibrin constructs where cells can directly adhere to the hydrogel. To test this hypothesis, MSCs were encapsulated in both agarose and fibrin hydrogels and were cultured for 21 days in free swelling (FS) or dynamically compressed (DC) conditions. While the effect of TGF-β3 concentration coupled with DC was investigated, no significant interactions were found. DC exerted a similar response with 1 ng/mL TGF-β3 as with 10 ng/mL TGF-β3; consequently only the 10 ng/mL TGF-β3 condition is presented. Cell viability was unaffected by DC (data not shown). DC inhibited sGAG ($p<0.0001$) and total collagen ($p<0.0001$) accumulation in both agarose and fibrin constructs (Fig. 3A). Both collagen type I and type II staining intensities were reduced in response to DC (Fig. 3C). Furthermore, DC acted to inhibit collagen type X staining in agarose (Fig. 3C); leading to a subsequent inhibition of calcific deposits demonstrated through the absence of alizarin red stain (Fig. 3B). As stated above, no evidence of mineralisation was observed in fibrin constructs (Fig. 3B). In contrast, DC acted to increase ALP activity in both agarose and fibrin encapsulated MSCs as indicated by enzyme secretion to the media ($p=0.0001$; Fig. 3A) and histochemical staining (Fig. 3B). As DC also suppressed cartilage-specific matrix accumulation and mineralisation in agarose, one could infer that increased ALP activity in the absence of robust chondrogenesis is not indicative of an endochondral phenotype. In addition to inhibiting chondrogenic and endochondral

differentiation, DC repressed myogenesis. Though intense α-smooth muscle actin staining was present around the periphery of FS fibrin constructs, DC acted to completely inhibit this myogenic marker (Fig. 3C). Consequently, we were unable to provide support for our initial hypothesis that dynamic compression would not suppress differentiation of MSCs embedded in fibrin constructs where cells can directly adhere to the hydrogel.

3.3 Extrinsic mechanical stimuli determine the eventual chondrogenic versus myogenic fate decision in MSC seeded fibrin constructs

Fibrin appeared to initially support both a chondrogenic and a myogenic phenotype. Given that the mechanically loaded environment of a fibrin clot within an osteochondral defect and other *in vivo* regenerative environments often supports a chondrogenic phenotype, it was hypothesised that in the long-term, dynamic compression could direct MSCs toward a chondrogenic as opposed to a myogenic phenotype. This hypothesis was partially motivated by our previous studies which demonstrated that the application of dynamic compression to agarose encapsulated MSCs following 3 weeks of TGF-β3 induced differentiation enhances subsequent chondrogenesis (Haugh et al., 2011; Thorpe et al., 2010). To further probe the effect of dynamic compression on differentiation within fibrin hydrogels, constructs were harvested for analysis of gene expression using real time RT-PCR after 21 days in FS or DC culture with 10 ng/mL TGF-β3. DC of fibrin encapsulated MSCs had no effect on the chondrogenic genes Sry-related high mobility group box-9 (SOX9) and aggrecan (ACAN; Fig. 4). However, DC did up-regulate collagen type II (COL2A1) gene expression relative to FS controls (p=0.0011; Fig. 4). Gene expression for collagen type X (COL10A1), an endochondral marker, was expressed at low levels and was not modulated by DC (Fig. 4). This correlated with negative immuno staining for collagen type X in fibrin (Fig. 2C). Collagen type I (COL1A1), a marker of both osteogenic and myogenic differentiation was

down regulated in response to dynamic compression (p=0.0004; Fig. 4). Expression of myogenic markers, α-smooth muscle actin (ACTA2) and calponin-1 (CNN1) were strongly down-regulated in DC fibrin constructs (p=0.0001 & p=0.0286 respectively; Fig. 4); suggesting that DC inhibits myogenic differentiation. Gene expression of heavy chain myosin-1, a late marker of myogenic differentiation, was expressed at low levels in both FS and DC groups.

We next explored how such changes in gene expression would impact markers of differentiation in the long-term. MSCs encapsulated in fibrin hydrogels were cultured for 42 days with 10 ng/mL TGF-β3. Dynamically compressed (DC) constructs were subjected to daily dynamic compression from day 0 to day 42, while delayed dynamically compressed (DDC) constructs were cultured in FS conditions up to day 21, when daily dynamic compression was initiated and continued until day 42. Dynamic compression from day 0 (DC) led to an increase in the rate of sGAG accumulation from day 21 to day 42 compared to FS controls (p<0.01, Fig. 5A), such that total accumulation was comparable to FS controls by day 42 (Fig. 5A). Initiation of dynamic compression at day 21 (DDC) had a positive effect on sGAG accumulation such that it was greater than both FS (p=0.0189) and DC (p=0.0356) constructs by day 42 (Fig. 5A). Immunofluorescent staining for collagen type II at day 42 was markedly more intense for DC constructs than either FS or DDC constructs (Fig. 5C), correlating with the up-regulation of COL2A1 gene expression in response to dynamic compression at day 21 (Fig. 4). Moreover, collagen type II immunofluorescent staining was more intense in DDC constructs compared to FS controls which were negative for this chondrogenic marker (Fig 5C).

As described above, long-term FS culture in fibrin hydrogels appeared to encourage a myogenic phenotype; apparent with strong staining for both α-smooth muscle actin and type I collagen (Fig. 5C). DC acted to inhibit myogenic differentiation. DC constructs had a larger

diameter than FS constructs at day 42 (p=0.0208) suggesting that DC suppresses cell-mediated contraction, typical of myogenic differentiation. Collagen type I immunofluorescence was also reduced in DC constructs compared to both FS and DDC constructs at day 42 (Fig. 5C), while DC constructs stained negatively for α-smooth muscle actin (Fig. 5C). DDC constructs did exhibit faint staining close to the construct edge (Fig. 5C).

Although the total ALP secreted at day 42 did not differ across dynamic compression conditions, the temporal patterns of ALP secretion did (Fig. 5A). ALP secretion increased between days 21-42 compared with the first 21 days for FS (p=0.0002) and DDC (p=0.0004) constructs (Fig. 5A), while it decreased for DC constructs between days 21-42 (p<0.0001; Fig. 5A). In spite of this, there were no discernible differences in ALP enzyme activity staining across dynamic compression conditions (Fig. 5B) and all constructs stained negatively for both collagen type X and calcific deposition (not shown).

4. Discussion

The aim of the study was to explore how cell-matrix interactions and the external mechanical environment interact to regulate stem cell fate in response to TGF-β3. Agarose was found to support a spherical cell morphology and a chondrogenic phenotype, while fibrin facilitated a spread cell morphology, cell-cell interactions and stress fibre formation. Initially fibrin constructs stained positively for both chondrogenic and myogenic markers, but in the long-term this substrate supported a more myogenic phenotype; evident by strong staining for α-smooth muscle actin and the absence of type II collagen staining after 6 weeks of FS culture. However, the ultimate fate decision of the MSCs was not determined by the specific characteristics of the local substrate, but rather by the external mechanical environment. Initially dynamic compression suppressed differentiation along either pathway, but in the

long-term these mechanical signals directed the MSCs along a chondrogenic pathway as opposed to the default myogenic route supported by the uncompressed fibrin clot.

In a free swelling environment, the fate decision of MSCs was determined by the local substrate. Unlike agarose (to which cells cannot directly adhere), fibrin facilitates integrin mediated cellular attachment through two pairs of RGD sites (Cheresh et al., 1989). Chondrogenic differentiation of MSCs has previously been shown to be repressed within RGD-modified agarose hydrogels (Connelly et al., 2008). More robust chondrogenesis was observed in agarose constructs where cells assumed a spherical morphology; while myogenesis was suppressed within these hydrogels. In contrast, myogenic differentiation was evident in fibrin constructs where MSCs took on a well spread morphology, with evidence of cell-cell interactions and the formation of F-actin stress fibres resulting in significant cell mediated hydrogel contraction. This is in general agreement with the findings of Gao *et al.* (2010) who demonstrated using micropatterned substrates that a rounded cell shape led to an up-regulation of chondrogenic genes while a spread cell shape led to an up-regulation of myogenic genes in the presence of TGF-β3.

To the best of our knowledge, differences between the two hydrogel types other than the availability of binding sites are less likely to explain the observed differences in MSC fate in free swelling conditions. The agarose hydrogels used in this study were stiffer than the fibrin hydrogels (Dynamic modulus: Agarose 50 kPa; Fibrin 31 kPa). While hydrogel modulus is a known regulator of stem cell fate when RGD binding sites are available (Huebsch et al., 2010), to the best of our knowledge there is no evidence to suggest that these differences in stiffness between agarose and fibrin constructs, in isolation, would explain our findings. Furthermore, no evidence of MSC differentiation was observed in constructs not supplemented with TGF-β3 (data not shown), suggesting that any soluble factors present in

the fibrin itself are unlikely to be driving the observed differences in MSC fate between the two hydrogels.

Chondrogenically primed bone marrow MSCs have been shown to eventually undergo hypertrophy and endochondral ossification (Farrell et al., 2009; Hellingman et al., 2010; Pelttari et al., 2006). The agarose hydrogels appeared to support an endochondral pathway for encapsulated MSCs, apparent in type X collagen staining, ALP activity and calcific deposits. No evidence of mineralisation or collagen type X was observed in fibrin constructs, suggesting that fibrin encapsulated MSCs may not have progressed sufficiently along the chondrogenic pathway to enable further differentiation toward an endochondral phenotype.

Dynamic compression, initiated at the onset of differentiation, suppressed markers associated with the chondrogenic, myogenic and endochondral phenotypes. Suppression of chondrogenesis with dynamic compression in agarose hydrogels has been previously observed (Huang et al., 2010; Mouw et al., 2007; Thorpe et al., 2008). Both chondrogenic and osteogenic differentiation markers have been shown to be reduced in response to dynamic compression for MSCs encapsulated in RGD modified poly(ethylene glycol) hydrogels (Steinmetz and Bryant, 2011). Furthermore, dynamic compression has been shown to inhibit cartilage specific matrix production in chondrocyte seeded fibrin hydrogels (Hunter et al., 2004). The only marker increased by dynamic compression in the short-term in this study was ALP enzyme activity. This has been proposed as an *in vitro* marker suggestive of subsequent calcification (Dickhut et al., 2009), however in this case, increased ALP activity did not translate to calcification. Dynamic compression may be suppressing mineralisation through inhibition of chondrogenesis and the subsequent progression along the endochondral pathway. Alternatively, dynamic compression could be preventing differentiation towards hypertrophy, helping to maintain a more stable chondrogenic phenotype. Previous studies

have provided support for the hypothesis that mechanical cues suppress hypertrophy of chondrogenically primed MSCs (Bian et al., 2012; Steward et al., 2012; Vinardell et al., 2012).

While dynamic compression initially suppressed chondrogenesis in fibrin hydrogels, long-term dynamic compression was associated with increased expression of type II collagen. sGAG and total collagen accumulation increased between day 21 and 42 in response to continued dynamic compression while a concurrent decrease in ALP activity was observed. Moreover, accumulated collagen was predominantly collagen type II, in agreement with increased gene expression at day 21. Most noticeable however was the complete suppression of α-smooth muscle actin staining and the less intense collagen type I staining, as well as the down-regulation of α-smooth muscle actin (ACTA2) and calponin-1 (CNN1) gene expression, demonstrating that external mechanical loading was driving the MSC fate decision in fibrin constructs. At this stage the molecular mechanism through which dynamic compression regulates the myogenic versus chondrogenic fate decision in fibrin hydrogels is unclear. Cell shape has been shown to regulate this fate decision (Gao et al., 2010), although there was no strong evidence to suggest that dynamic compression is leading to a more spherical cell morphology in fibrin hydrogels. Gao *et al.* (2010) demonstrated that TGF-β3 activated Rac1 and increased N-cadherin expression in spread cells, leading to the up-regulation of myogenic genes. Dynamic compression could possibly impact at any point along this signalling cascade. For example, dynamic compression could potentially reduce the expression of N-cadherin or alter associations with N-cadherin at the cell membrane, such as N-cadherin and β-catenin association, which has previously been shown to be mechano-regulated (Arnsdorf et al., 2009). If this were indeed the case, it could potentially explain the temporal response of MSCs to loading. N-cadherin is required for the initial cellular condensation at the onset of chondrogenesis (Oberlender and Tuan, 1994a), but its expression

diminishes as differentiation along this pathway progresses (Oberlender and Tuan, 1994b). If dynamic compression inhibits N-cadherin expression, it may explain the initial suppression of both myogenesis and chondrogenesis, leading to the long-term promotion of a chondrogenic phenotype. Further work is required to elucidate the molecular mechanism involved in this stem cell fate decision in response to dynamic compression.

In conclusion, we have shown that MSC differentiation in response to TGF-β stimulation is dependent upon the hydrogel within which the cells are encapsulated. Perhaps more importantly, this study demonstrates that cues present in the *in vivo* environment, such as extrinsic mechanical load, can override the influence of specific substrates, scaffolds or hydrogels that have been shown to modulate stem fate in an *in vitro* setting. The temporal data presented in this study highlight the importance of considering how MSCs respond to extrinsic mechanical signals in the long term. In the context of stem cell based therapies for tissue regeneration, it may be that the site specific mechanical environment is the ultimate regulator of phenotype and function.

Conflict of Interest

The authors have no conflict of interest.

Acknowledgements

Funding was provided by Science Foundation Ireland (President of Ireland Young Researcher Award: 08/YI5/B1336) and the European Research Council (StemRepair – Project number 258463). We thank Ms Rebecca Rolfe for assistance with qPCR.

References

Arnsdorf EJ, Tummala P, Jacobs CR, 2009. Non-canonical Wnt signaling and N-cadherin related beta-catenin signaling play a role in mechanically induced osteogenic cell fate. PLoS One 4, e5388.

Bian L, Zhai DY, Zhang EC, Mauck RL, Burdick JA, 2012. Dynamic compressive loading enhances cartilage matrix synthesis and distribution and suppresses hypertrophy in hMSC-laden hyaluronic acid hydrogels. Tissue Eng Part A 18, 715-724.

Buckley CT, Thorpe SD, O'Brien FJ, Robinson AJ, Kelly DJ, 2009. The effect of concentration, thermal history and cell seeding density on the initial mechanical properties of agarose hydrogels. J Mech Behav Biomed Mater 2, 512-521.

Campbell JJ, Lee DA, Bader DL, 2006. Dynamic compressive strain influences chondrogenic gene expression in human mesenchymal stem cells. Biorheology 43, 455-470.

Caplan AI, 1991. Mesenchymal stem cells. J Orthop Res 9, 641-650.

Carter DR, Blenman PR, Beaupre GS, 1988. Correlations between mechanical stress history and tissue differentiation in initial fracture healing. J Orthop Res 6, 736-748.

Catelas I, Sese N, Wu BM, Dunn JC, Helgerson S, Tawil B, 2006. Human mesenchymal stem cell proliferation and osteogenic differentiation in fibrin gels in vitro. Tissue Eng 12, 2385-2396.

Cheresh DA, Berliner SA, Vicente V, Ruggeri ZM, 1989. Recognition of distinct adhesive sites on fibrinogen by related integrins on platelets and endothelial cells. Cell 58, 945-953.

Connelly JT, Garcia AJ, Levenston ME, 2008. Interactions between integrin ligand density and cytoskeletal integrity regulate BMSC chondrogenesis. J Cell Physiol 217, 145-154.

Dickhut A, Pelttari K, Janicki P, Wagner W, Eckstein V, Egermann M, Richter W, 2009. Calcification or dedifferentiation: requirement to lock mesenchymal stem cells in a desired differentiation stage. J Cell Physiol 219, 219-226.

Engler AJ, Sen S, Sweeney HL, Discher DE, 2006. Matrix elasticity directs stem cell lineage specification. Cell 126, 677-689.

Farrell E, et al., 2009. Chondrogenic priming of human bone marrow stromal cells: a better route to bone repair? Tissue Eng Part C Methods 15, 285-295.

Gao L, McBeath R, Chen CS, 2010. Stem cell shape regulates a chondrogenic versus myogenic fate through Rac1 and N-cadherin. Stem Cells 28, 564-572.

Haugh MG, Meyer EG, Thorpe SD, Vinardell T, Duffy GP, Kelly DJ, 2011. Temporal and Spatial Changes in Cartilage-Matrix-Specific Gene Expression in Mesenchymal Stem Cells in Response to Dynamic Compression. Tissue Eng Part A 17, 3085-3093.

Hellingman CA, Koevoet W, Kops N, Farrell E, Jahr H, Liu W, Baatenburg de Jong RJ, Frenz DA, van Osch GJ, 2010. Fibroblast growth factor receptors in in vitro and in vivo chondrogenesis: relating tissue engineering using adult mesenchymal stem cells to embryonic development. Tissue Eng Part A 16, 545-556.

Huang AH, Farrell MJ, Kim M, Mauck RL, 2010. Long-term dynamic loading improves the mechanical properties of chondrogenic mesenchymal stem cell-laden hydrogel. Eur Cell Mater 19, 72-85.

Huang CY, Hagar KL, Frost LE, Sun Y, Cheung HS, 2004. Effects of cyclic compressive loading on chondrogenesis of rabbit bone-marrow derived mesenchymal stem cells. Stem Cells 22, 313-323.

Huebsch N, Arany PR, Mao AS, Shvartsman D, Ali OA, Bencherif SA, Rivera-Feliciano J, Mooney DJ, 2010. Harnessing traction-mediated manipulation of the cell/matrix interface to control stem-cell fate. Nat Mater 9, 518-526.

Hunter CJ, Mouw JK, Levenston ME, 2004. Dynamic compression of chondrocyte-seeded fibrin gels: effects on matrix accumulation and mechanical stiffness. Osteoarthritis Cartilage 12, 117-130.

Ignat'eva NY, Danilov NA, Averkiev SV, Obrezkova MV, Lunin VV, Sobol EN, 2007. Determination of hydroxyproline in tissues and the evaluation of the collagen content of the tissues. J Anal Chem 62, 51-57.

Janmey PA, Winer JP, Weisel JW, 2009. Fibrin gels and their clinical and bioengineering applications. J R Soc Interface 6, 1-10.

Jeon ES, Moon HJ, Lee MJ, Song HY, Kim YM, Bae YC, Jung JS, Kim JH, 2006. Sphigosylphosphorylcholine induces differentiation of human mesenchymal stem cells into smooth-muscle-like through a TGF-β-dependent mechanism. Journal of Cell Science 119, 4994-5005.

Johnstone B, Hering TM, Caplan AI, Goldberg VM, Yoo JU, 1998. In vitro chondrogenesis of bone marrow-derived mesenchymal progenitor cells. Exp Cell Res 238, 265-272.

Kafienah W, Sims TJ, 2004. Biochemical methods for the analysis of tissue-engineered cartilage. Methods Mol Biol 238, 217-230.

Kim YJ, Sah RL, Doong JY, Grodzinsky AJ, 1988. Fluorometric assay of DNA in cartilage explants using Hoechst 33258. Anal Biochem 174, 168-176.

Kinner B, Zaleskas JM, Spector M, 2002. Regulation of smooth muscle actin expression and contraction in adult human mesenchymal stem cells. Experimental Cell Research 278, 72-83.

Kisiday JD, Frisbie DD, McIlwraith CW, Grodzinsky AJ, 2009. Dynamic compression stimulates proteoglycan synthesis by mesenchymal stem cells in the absence of chondrogenic cytokines. Tissue Eng Part A 15, 2817-2824.

Kock LM, Schulz RM, van Donkelaar CC, Thummler CB, Bader A, Ito K, 2009. RGD-dependent integrins are mechanotransducers in dynamically compressed tissue-engineered cartilage constructs. J Biomech 42, 2177-2182.

Kundu AK, Khatiwala CB, Putnam AJ, 2009. Extracellular matrix remodeling, integrin expression, and downstream signaling pathways influence the osteogenic differentiation of mesenchymal stem cells on poly(lactide-co-glycolide) substrates. Tissue Eng Part A 15, 273-283.

Li Z, Kupcsik L, Yao SJ, Alini M, Stoddart MJ, 2009. Chondrogenesis of human bone marrow mesenchymal stem cells in fibrin-polyurethane composites. Tissue Eng Part A 15, 1729-1737.

Li Z, Kupcsik L, Yao SJ, Alini M, Stoddart MJ, 2010. Mechanical load modulates chondrogenesis of human mesenchymal stem cells through the TGF-beta pathway. J Cell Mol Med 14, 1338-1346.

Livak KJ, Schmittgen TD, 2001. Analysis of relative gene expression data using real-time quantitative PCR and the 2(-Delta Delta C(T)) Method. Methods 25, 402-408.

Mackay AM, Beck SC, Murphy JM, Barry FP, Chichester CO, Pittenger MF, 1998. Chondrogenic differentiation of cultured human mesenchymal stem cells from marrow. Tissue Eng 4, 415-428.

Mauck RL, Byers BA, Yuan X, Tuan RS, 2007. Regulation of cartilaginous ECM gene transcription by chondrocytes and MSCs in 3D culture in response to dynamic loading. Biomech Model Mechanobiol 6, 113-125.

McBeath R, Pirone DM, Nelson CM, Bhadriraju K, Chen CS, 2004. Cell shape, cytoskeletal tension, and RhoA regulate stem cell lineage commitment. Dev Cell 6, 483-495.

Miao D, Scutt A, 2002. Histochemical localization of alkaline phosphatase activity in decalcified bone and cartilage. J Histochem Cytochem 50, 333-340.

Minguell JJ, Erices A, Conget P, 2001. Mesenchymal stem cells. Exp Biol Med (Maywood) 226, 507-520.

Mouw JK, Connelly JT, Wilson CG, Michael KE, Levenston ME, 2007. Dynamic compression regulates the expression and synthesis of chondrocyte-specific matrix molecules in bone marrow stromal cells. Stem Cells 25, 655-663.

Nieponice A, Maul TM, Cumer JM, Soletti L, Vorp DA, 2007. Mechanical stimulation induces morphological and phenotypic changes in bone marrow-derived progenitor cells within a three-dimensional fibrin matrix. Journal of Biomedical Materials Research Part A 81A, 523-530.

O'Cearbhaill ED, Murphy M, Barry F, McHugh PE, Barron V, 2010. Behavior of human mesenchymal stem cells in fibrin-based vascular tissue engineering constructs. Ann Biomed Eng 38, 649-657.

Oberlender SA, Tuan RS, 1994a. Expression and functional involvement of N-cadherin in embryonic limb chondrogenesis. Development 120, 177-187.

Oberlender SA, Tuan RS, 1994b. Spatiotemporal profile of N-cadherin expression in the developing limb mesenchyme. Cell Adhes Commun 2, 521-537.

Park JS, Chu JS, Tsou AD, Diop R, Tang Z, Wang A, Li S, 2011. The effect of matrix stiffness on the differentiation of mesenchymal stem cells in response to TGF-beta. Biomaterials 32, 3921-3930.

Pauwels F, 1960. A new theory on the influence of mechanical stimuli on the differentiation of supporting tissue. The tenth contribution to the functional anatomy and causal morphology of the supporting structure. Z Anat Entwicklungsgesch 121, 478-515.

Pelaez D, Charles Huang CY, Cheung HS, 2009. Cyclic compression maintains viability and induces chondrogenesis of human mesenchymal stem cells in fibrin gel scaffolds. Stem Cells and Development 18, 93-102.

Pelttari K, Winter A, Steck E, Goetzke K, Hennig T, Ochs BG, Aigner T, Richter W, 2006. Premature induction of hypertrophy during in vitro chondrogenesis of human mesenchymal stem cells correlates with calcification and vascular invasion after ectopic transplantation in SCID mice. Arthritis Rheum 54, 3254-3266.

Pittenger MF, Mackay AM, Beck SC, Jaiswal RK, Douglas R, Mosca JD, Moorman MA, Simonetti DW, Craig S, Marshak DR, 1999. Multilineage potential of adult human mesenchymal stem cells. Science 284, 143-147.

Prendergast PJ, Huiskes R, Soballe K, 1997. ESB Research Award 1996. Biophysical stimuli on cells during tissue differentiation at implant interfaces. J Biomech 30, 539-548.

Steinmetz NJ, Bryant SJ, 2011. The effects of intermittent dynamic loading on chondrogenic and osteogenic differentiation of human marrow stromal cells encapsulated in RGD-modified poly(ethylene glycol) hydrogels. Acta Biomater 7, 3829-3840.

Steward AJ, Thorpe SD, Vinardell T, Buckley CT, Wagner DR, Kelly DJ, 2012. Cell-matrix interactions regulate mesenchymal stem cell response to hydrostatic pressure. Acta Biomater 8, 2153-2159.

Thorpe SD, Buckley CT, Vinardell T, O'Brien FJ, Campbell VA, Kelly DJ, 2008. Dynamic compression can inhibit chondrogenesis of mesenchymal stem cells. Biochem Biophys Res Commun 377, 458-462.

Thorpe SD, Buckley CT, Vinardell T, O'Brien FJ, Campbell VA, Kelly DJ, 2010. The response of bone marrow-derived mesenchymal stem cells to dynamic compression following tgf-β3 induced chondrogenic differentiation. Ann Biomed Eng 38, 2896-2909.

Vinardell T, Rolfe RA, Buckley CT, Meyer EG, Ahearne M, Murphy P, Kelly DJ, 2012. Hydrostatic pressure acts to stabilise a chondrogenic phenotype in porcine joint tissue derived stem cells. Eur Cell Mater 23, 121-132; discussion 133-134.

Wang QG, Magnay JL, Nguyen B, Thomas CR, Zhang Z, El Haj AJ, Kuiper NJ, 2009. Gene expression profiles of dynamically compressed single chondrocytes and chondrons. Biochem Biophys Res Commun 379, 738-742.

Weinand C, Pomerantseva I, Neville CM, Gupta R, Weinberg E, Madisch I, Shapiro F, Abukawa H, Troulis MJ, Vacanti JP, 2006. Hydrogel-beta-TCP scaffolds and stem cells for tissue engineering bone. Bone 38, 555-563.

Table/Figure Legends

Table 1: Peak stress at 10% strain, equilibrium and 1 Hz dynamic moduli of agarose and fibrin hydrogels seeded with MSCs at 15×10^6 cells/mL. An unconfined stress-relaxation test was carried out with a ramp to 10% strain at 1 μm/s followed by 30 min. relaxation with subsequent cyclic testing from 10% to 11% strain at 1 Hz. *: $p<0.001$ vs. Fibrin.

Table 2: Primary antibodies and controls used for immunohistochemistry.

Table 3: TaqMan® primer/probes used for real-time PCR.

Figure 1. MSC seeded agarose and fibrin constructs were cultured for 21 days in FS (unloaded) conditions with the addition of either 1 ng/mL or 10 ng/mL TGF-β3. Cytoskeletal F-actin filaments in day 21 constructs were stained with rhodamine 110 conjugated phalloidin. ($n = 2$) Scale bar: 20 μm.

Figure 2. The influence of hydrogel substrate and TGF-β3 concentration on markers of chondrogenic, endochondral and myogenic differentiation after 21 days culture. A: sGAG (top) and total collagen (middle) construct biochemical content, and alkaline phosphatase (ALP) secreted to the media (bottom) ($n = 4$). B: Histological staining of constructs with alcian blue for sulphated mucins, picro sirius red for total collagen, naphthol phosphate with fast red for ALP enzyme activity and alizarin red for calcific deposition ($n = 2$). C: Immunofluorescent staining for collagen type I, collagen type II, collagen type X and α-smooth muscle actin (green) with nucleus counterstained with DAPI (blue) ($n = 2$). Scale bar: 500 μm; inset scale bar: 50 μm.

Figure 3. The influence of dynamic compression and hydrogel substrate on markers of MSC chondrogenic, endochondral and myogenic differentiation after 21 days culture with 10 ng/mL TGF-β3. A: sGAG (top) and total collagen (middle) construct biochemical content, and alkaline phosphatase (ALP) secreted to the media (bottom) (n = 4). B: Histological staining of constructs with alcian blue for sulphated mucins, picro sirius red for total collagen, naphthol phosphate with fast red for ALP enzyme activity and alizarin red for calcific deposition (n = 2). C: Immunofluorescent staining for collagen type I, collagen type II, collagen type X and α-smooth muscle actin (green) with nucleus counterstained with DAPI (blue) (n =2). Scale bar: 500 μm; inset scale bar: 50 μm.

Figure 4. Dynamic compression was applied to fibrin encapsulated MSCs in the presence of 10 ng/mL TGF-β3 for 21 days with chondrogenic, myogenic and endochondral gene expression assessed at day 21. Dynamically compressed construct gene expression is presented relative to the free-swelling control. FS: Free-swelling; DC: Dynamic compression (n = 4).

Figure 5. The influence of long-term dynamic compression on markers of MSC chondrogenic and myogenic differentiation after 42 days culture in fibrin hydrogel with 10 ng/mL TGF-β3. A: sGAG accumulated (top), collagen accumulated (middle), and alkaline phosphatase (ALP) secreted to the media (bottom) from days 0-21, days 21-42 and days 0-42 (n = 4). B: Histological staining of constructs with alcian blue for sulphated mucins, picro sirius red for total collagen, and naphthol phosphate with fast red for ALP enzyme activity (n = 2). C: Immunofluorescent staining for collagen type I, collagen type II and α-smooth muscle actin (green) with nucleus counterstained with DAPI (blue) (n = 2). Scale bar: 500 μm; inset scale bar: 50 μm.

Figure 1

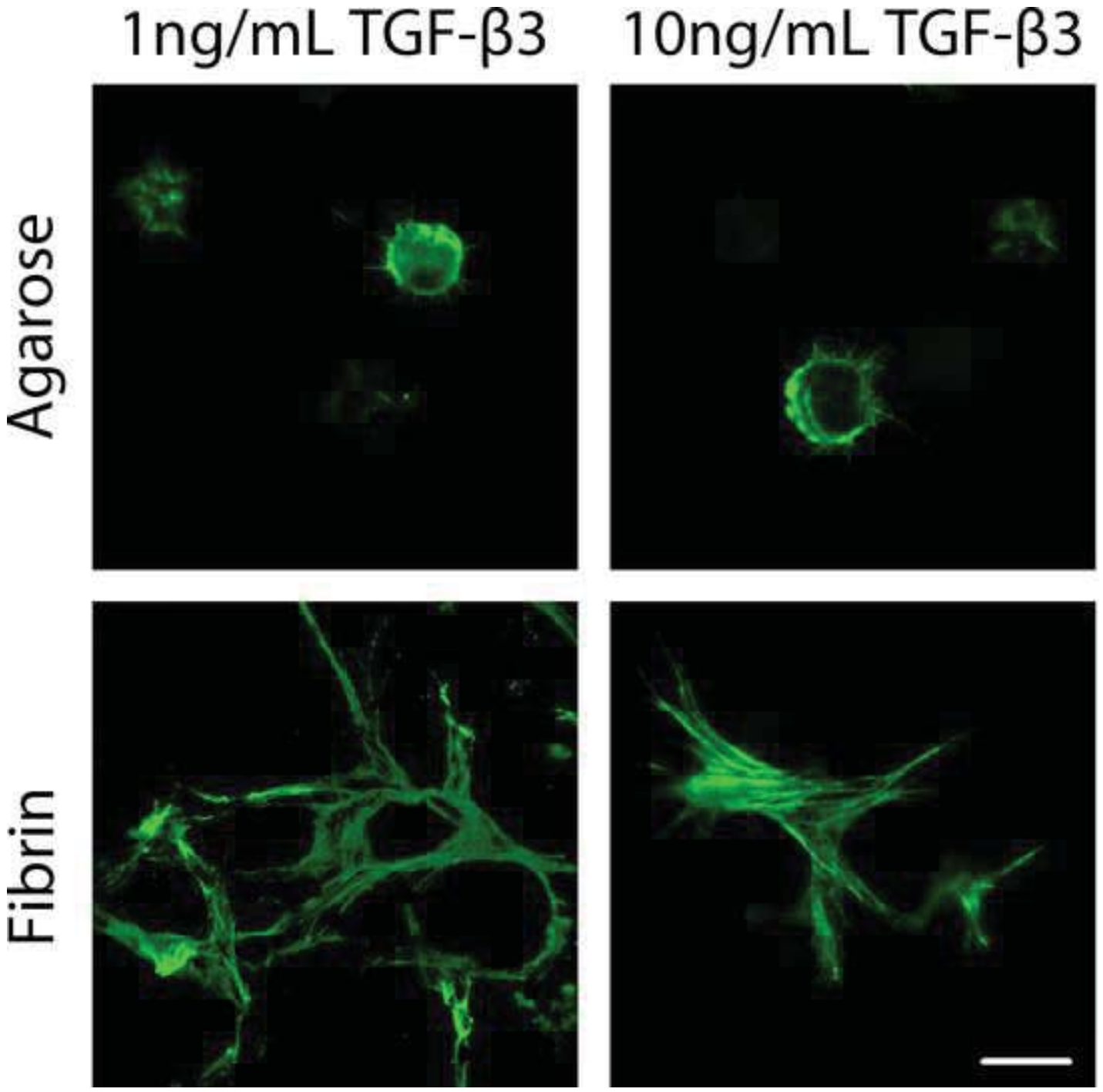

Figure 2

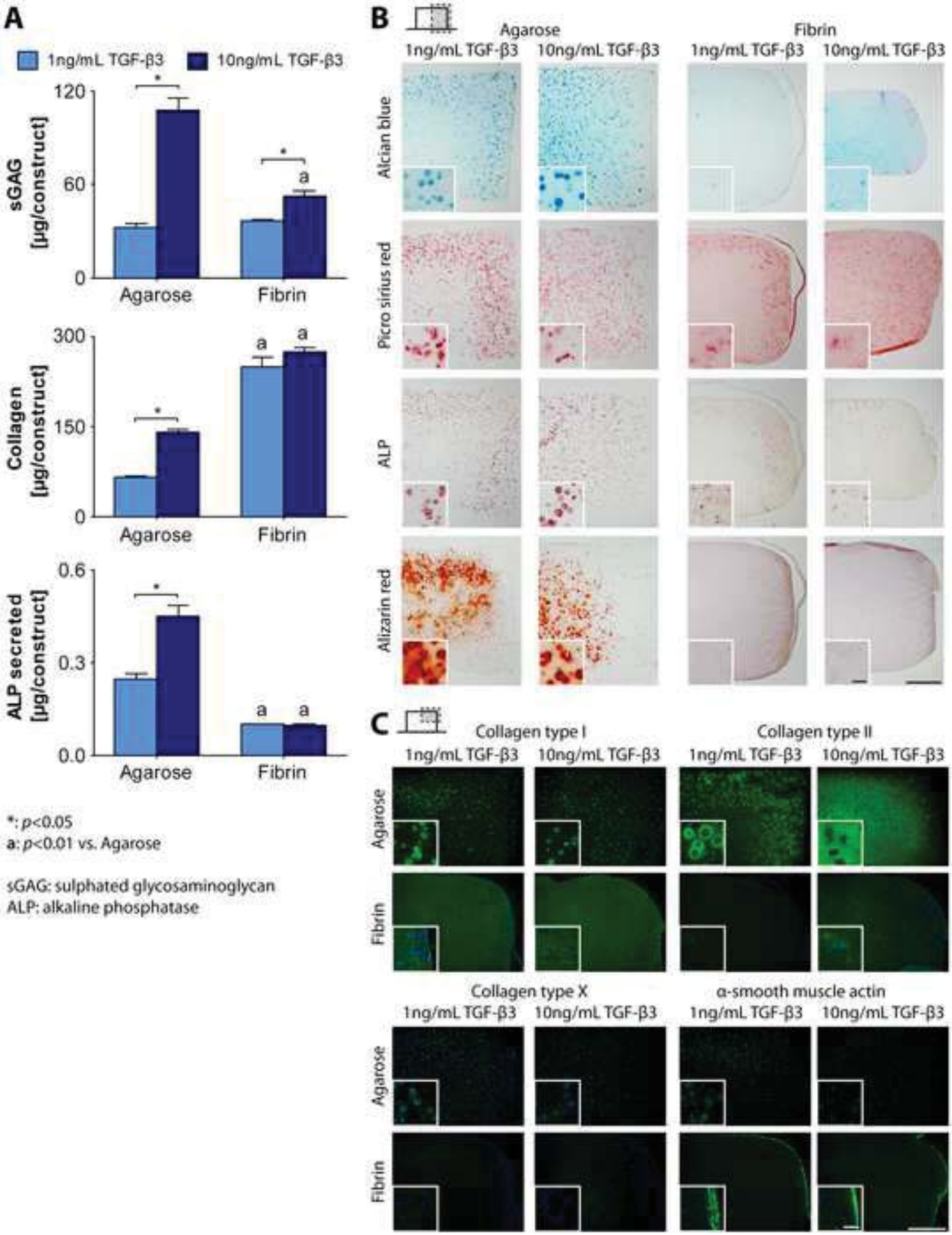
A
1ng/mL TGF-β3
10ng/mL TGF-β3
sGAG [µg/construct]
120
60
0
Agarose
Fibrin
a
Collagen [µg/construct]
300
150
0
ALP secreted [µg/construct]
0.6
0.3
0.0
*: p<0.05
a: p<0.01 vs. Agarose
sGAG: sulphated glycosaminoglycan
ALP: alkaline phosphatase
B
Agarose
Fibrin
Alcian blue
Picro sirius red
ALP
Alizarin red
C
Collagen type I
Collagen type II
Collagen type X
α-smooth muscle actin

Figure 3

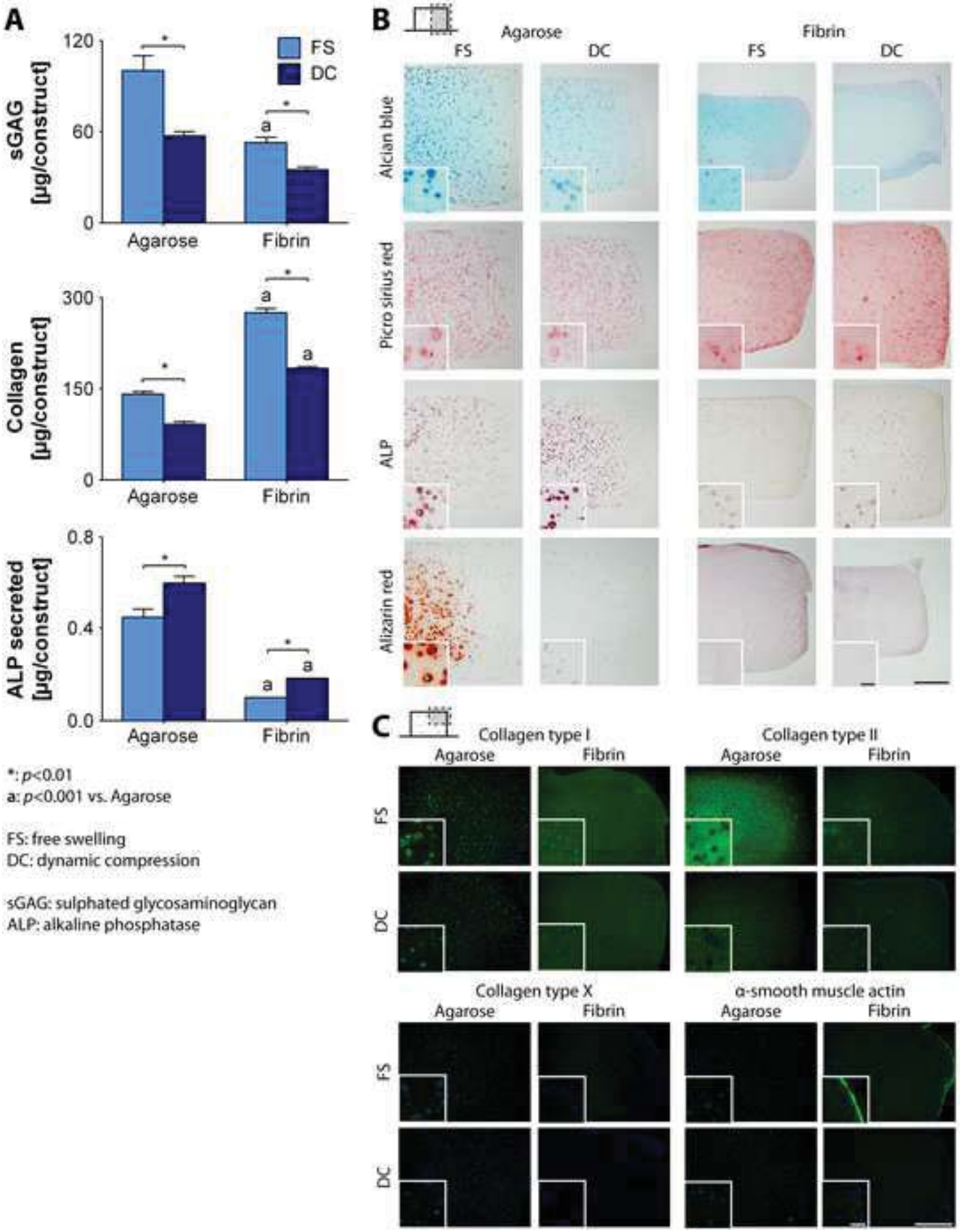

*: $p<0.01$
a: $p<0.001$ vs. Agarose

FS: free swelling
DC: dynamic compression

sGAG: sulphated glycosaminoglycan
ALP: alkaline phosphatase

Figure 4

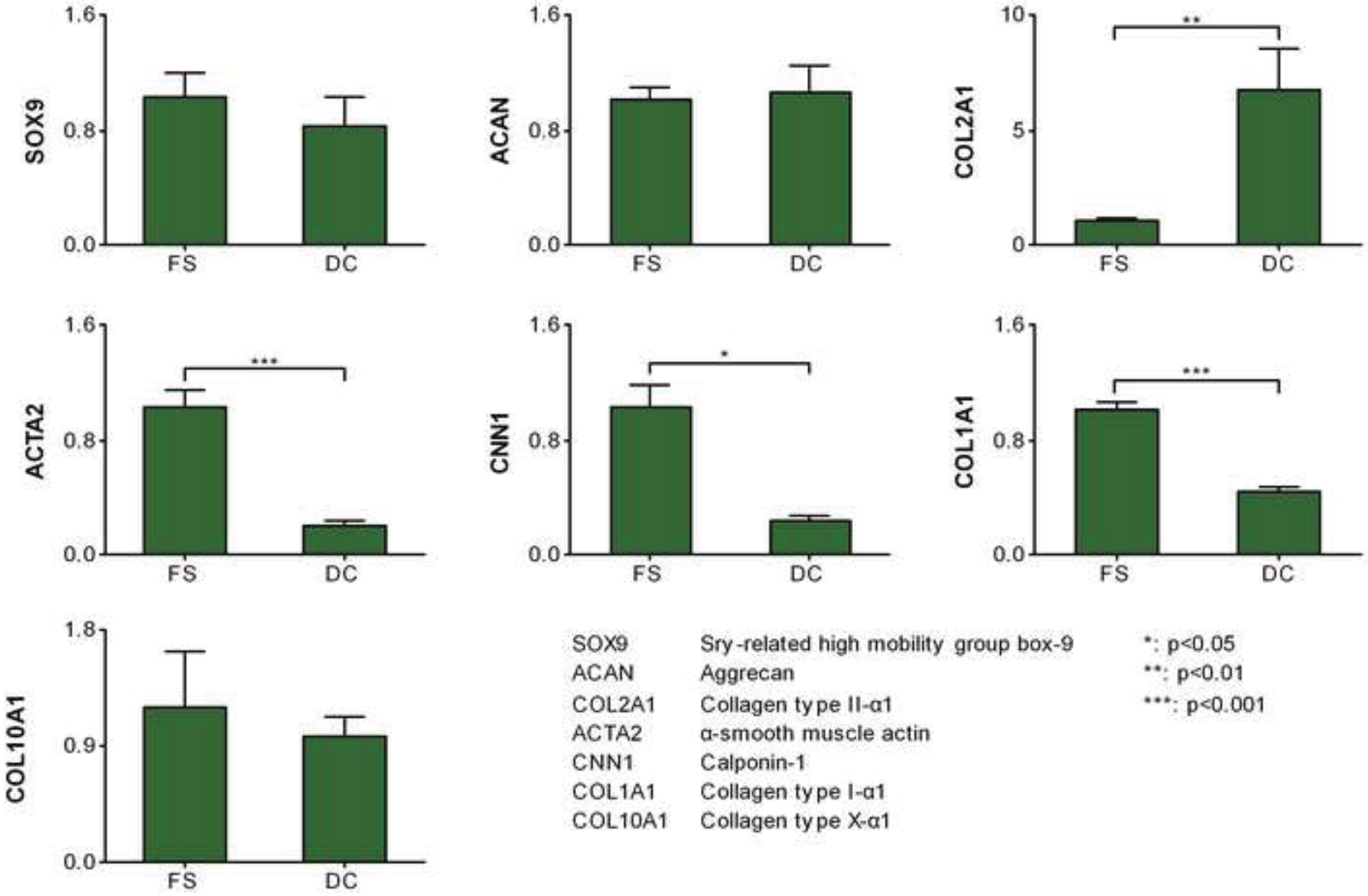
SOX9
1.6
0.8
0.0
FS
DC
ACAN
1.6
0.8
0.0
FS
DC
COL2A1
10
5
0
**
FS
DC
ACTA2
1.6
0.8
0.0
***
FS
DC
CNN1
1.6
0.8
0.0
*
FS
DC
COL1A1
1.6
0.8
0.0
***
FS
DC
COL10A1
1.8
0.9
0.0
FS
DC
SOX9 Sry-related high mobility group box-9
ACAN Aggrecan
COL2A1 Collagen type II-α1
ACTA2 α-smooth muscle actin
CNN1 Calponin-1
COL1A1 Collagen type I-α1
COL10A1 Collagen type X-α1
*: p<0.05
**: p<0.01
***: p<0.001

Figure 5

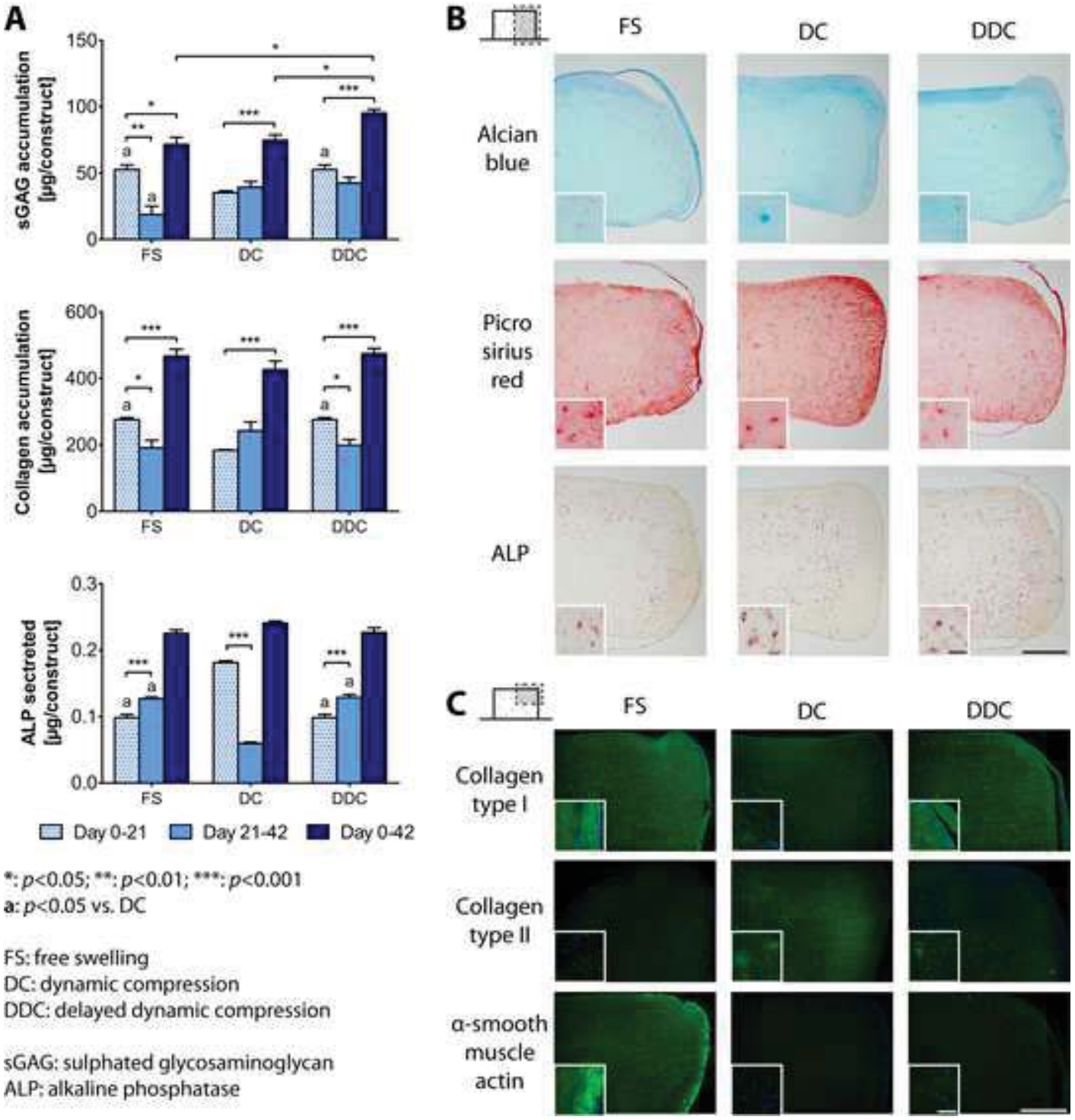

*: $p<0.05$; **: $p<0.01$; ***: $p<0.001$
a: $p<0.05$ vs. DC

FS: free swelling
DC: dynamic compression
DDC: delayed dynamic compression

sGAG: sulphated glycosaminoglycan
ALP: alkaline phosphatase

Table 1

Hydrogel	*Peak stress[kPa]*	*Equilibrium modulus [kPa]*	*1 Hz Dynamic modulus [kPa]*
Agarose	2.174±0.060	11.003±0.756*	49.981±0.741*
Fibrin	1.532±0.328	3.802±0.463	30.744±0.614

Table 2

Antigen	*Primary Antibody*	*Positive Control*	*Negative Control*
Collagen I	Monoclonal mouse (1:400; 1 mg/mL)	Porcine ligament	Porcine articular cartilage
Collagen II	Monoclonal mouse (1:100; 1 mg/mL)	Porcine articular cartilage	Porcine ligament
Collagen X	Monoclonal mouse (1:200; 1.4 mg/mL)	Porcine growth plate	Porcine ligament
α-smooth muscle actin	Monoclonal mouse (1:75; 0.2 mg/mL)	Porcine femoral artery	Porcine cartilage

Table 3

Gene Name	*Gene Symbol*	*Assay ID (Applied Biosystems)*	*Amplicon Length*
Glyceraldehyde-3-phosphate dehydrogenase	GAPDH	Ss03373286_u1	83
SRY (sex determining region Y)-box 9	SOX9	Ss03392406_m1	145
Aggrecan	ACAN	Ss03374822_m1	96
Collagen, type II, alpha 1	COL2A1	Ss03373344_g1	106
Actin, alpha 2, smooth muscle, aorta	ACTA2	Ss04245588_m1	84
Calponin 1, basic, smooth muscle	CNN1	Ss03392449_g1	83
Myosin, heavy chain 1, skeletal muscle, adult	MYH1	Ss03818758_s1	71
Collagen, type I, alpha 1	COL1A1	Ss03373340_m1	74
Collagen, type X, alpha 1	COL10A1	Ss03391766_m1	85

***Conflict of Interest Statement**

The authors have no conflict of interest.